IVYSPRING INTERNATIONAL PUBLISHER

Journal of Cancer

2017; 8(5): 839-851. doi: 10.7150/jca.17657

Research Paper

Gambogenic acid synergistically potentiates bortezomib-induced apoptosis in multiple myeloma

Runzhe Chen, Hongming Zhang, Ping Liu, Xue Wu, Baoan Chen✉

Department of Hematology and Oncology (Key Discipline of Jiangsu Medicine), Zhongda Hospital, Medical School, Southeast University, Nanjing 210009, Jiangsu Province, P.R. China

✉ Corresponding author: Baoan Chen, MD, PhD, Professor and director, Department of Hematology and Oncology, Zhongda Hospital, Medical School, Southeast University, Dingjiaqiao 87, Gulou District, Nanjing 210009, Jiangsu Province, P.R. China, Tel: 086 25 83272006 Fax: 086 25 83272011 E-mail: cba8888@hotmail.com

Received: 2016.09.21; Accepted: 2016.12.26; Published: 2017.03.07

Abstract

Background: Although the introduction of protease inhibitor bortezomib (BTZ) and immunomodulatory agent lenalidomide has led to improved outcomes in patients with multiple myeloma (MM), the disease remains incurable. Gambogenic acid (GNA), a polyprenylated xanthone isolated from the traditional Chinese medicine gamboge, has been reported to have potent antitumor activity and can effectively inhibit the survival and proliferation of cancer. In this study, we hypothesized that GNA could synergistically potentiate BTZ-induced apoptosis of MM cells and that combining BTZ and GNA may provide a more effective approach to treat MM. Hence, we investigate the *in vitro* and *in vivo* effects of BTZ and GNA, alone or in combination, against myeloma MM.1S cells.

Methods: Cell counting kit-8 (CCK-8) assay, combination index (CI) isobologram, flow cytometry, western blot, xenograft tumor models, terminal deoxynucleotidyl transferase dUTP nick end labeling (TUNEL) and immunochemistry were used in this study.

Results: The results showed that BTZ and GNA combination treatment resulted in a strong synergistic action against the MM.1S cell line. Increased G2/M phase cells were triggered by BTZ, GNA and the combined treatment. The combined treatment could induce more markedly apoptosis of MM.1S cells via the activation of PARP cleavage, P53, Caspase-3 cleavage and Bax and inhibition of Bcl-2 expression. An increased antitumor effects of combination therapy of BTZ and GNA on MM.1S xenograft models were observed, and combining BTZ and GNA was found to be superior to a single agent.

Conclusions: Our data support that a synergistic antitumor activity exists between BTZ and GNA, and provide a rationale for successful utilization of dual BTZ and GNA in MM chemotherapy in the future.

Key words: multiple myeloma, gambogenic acid, bortezomib, synergism, apoptosis

Introduction

Multiple myeloma (MM) is the most common primary tumor of the bone marrow that accounts for approximately 10% of all hematological cancer [1]. Over the last few decades, novel agents such as the proteasome inhibitor bortezomib (BTZ) (Figure 1A) and immunomodulatory agent thalidomide and lenalidomide have improved outcomes in MM patients. Many clinical trials of the second generations of these agents like pomalidomide, carfilzomib and ixazomib have also been conducted with better outcomes even in drug-resistant cases [2-7]. However, the general prognosis of MM is still unfavorable and a cure remains out of reach [8]. Moreover, severe side effects such as peripheral neuropathy and serious infections often occur in the majority of MM patients [9]. Therefore, the identification and validation of

novel targeted agents with less systemic toxicity is necessary to overcome drug resistance and to improve clinical outcomes of MM [3, 10].

In recent years, herbal and herbal-derived agents have been recognized as an attractive approach to cancer therapy [11-13]. There is evidence that various herbal medicines have proven to be useful and effective in sensitizing conventional agents, prolonging survival time, preventing side effects of chemotherapy and improving quality of life in cancer patients [14]. Gambogenic acid (GNA) (Figure 1A) is one of the natural compounds isolated from gamboge, a dry resin secreted from the garcinia hanburyi tree in Southeast Asia [15, 16]. Compared with more widely studied gambogic acid (GA), another compound isolated from gamboge, GNA has demonstrated advantages such as a more potent anticancer effect and less systemic toxicity according to early investigations [17-20]. The possible anticancer mechanisms of GNA are associated with the induction of apoptosis, enhancement of reactive oxygen species (ROS) accumulation, inhibition of telomerase activity and interception of MAPK signaling pathway [21-23]. Previous studies have shown that GNA could inhibit the growth of several types of human cancer cells, including cancers of the lung, prostate, gastric system, breast and liver *in vitro* and *in vivo*, but seldom have studies explored the role of GNA on MM [21-24]. Here, we asked whether this novel agent can improve the proteasome-based chemotherapy in MM by investigating the effects of GNA combined with BTZ with regard to their activities against MM *in vitro* and *in vivo* in this study.

Materials and methods

Cell culture

The human myeloma cell line, MM.1S was obtained from Nanjing Kebai Biotech. Co. Ltd. The cells were maintained in RPMI-1640 medium (Gibco, Grand Island, NY, USA) supplemented with 15% heat-inactivated fetal bovine serum (Sijiqing, Hangzhou, China), 100U/mL penicillin and 100lg/mL streptomycin (Sigma-Aldrich, St. Louis, MO, USA) in a humidified atmosphere of 5% CO_2 at 37°C. For hypoxia induction, cells were incubated in a sealed hypoxic chamber flushed with a gas mixture of 94% N_2, 5% CO_2 and 1% O_2.

Reagents

GNA (>98% purity, provided by Anhui University of Chinese Medicine, China) and BTZ (Selleck, Houston, TX, USA) were dissolved in dimethyl sulfoxide (DMSO) (Sigma Chemical Co., USA) to 100mM and stored at -20°C. Cell counting kit-8 (CCK-8) was purchased from Dojindo, Kumamoto, Japan and was dissolved in phosphate buffered saline (PBS). Annexin V-FITC Apoptosis Detection Kit was purchased from Becton, Dickinson and Company (USA). Terminal deoxynucleotidyl transferase dUTP nick end labeling (TUNEL) kit was provided by Guge, Wuhan, China. Antibodies against PARP, P53, Caspase-3, Bax and Bcl-2 were purchased from Cell Signaling Technology, Inc, USA.

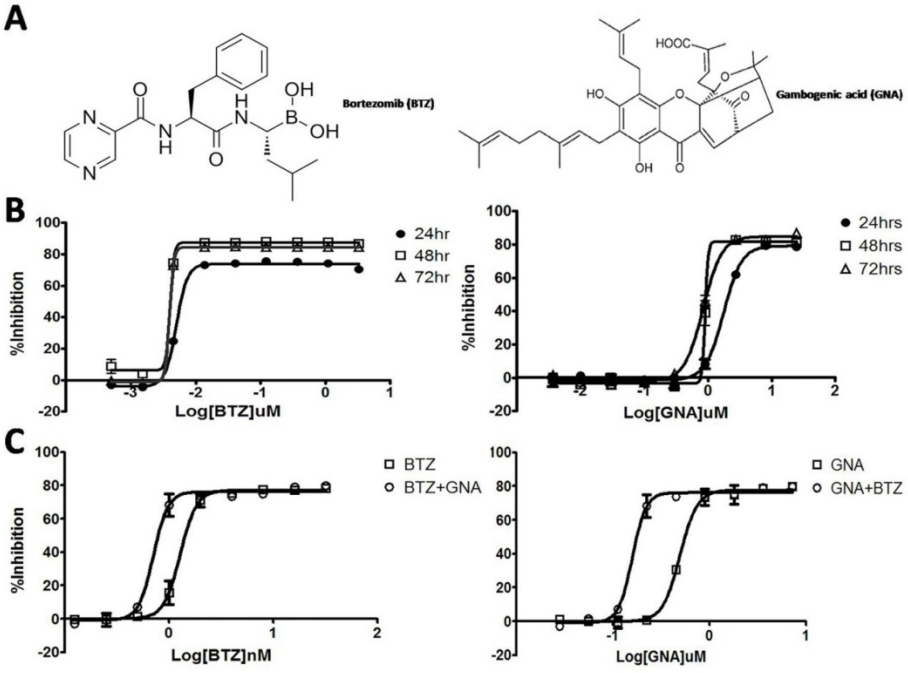

Figure 1. Effect of BTZ and GNA on the cell proliferation in MM.1S cells. (A) Chemical structure of BTZ and GNA. (B) Effect of BTZ or GNA as single agent inhibited the growth of MM.1S cells for 24, 48 and 72h, followed by analysis with CCK-8 assay. (C) Effect of combination of BTZ and GNA according to EC50 of MM.1S cells for 48h. These experiments were repeated in triplicate.

Cell proliferation assay and determination of combination index

The *in vitro* cell proliferation effects of BTZ and GNA alone were determined by CCK-8 assay. Briefly, cells were seeded onto 96-well plates at a density of 4×10^3 cells/well and treated with various concentrations of BTZ and GNA alone for 24, 48 and 72 hours respectively. The CCK-8 solution (10μL) was added to each well and incubated for an additional 4 hours. The absorbance was measured at 450nm using an ELX 800 Microplate Reader (BioTek Instruments, Inc, USA). Three wells were used for each concentration. The inhibitory rate of cell proliferation was calculated by the following formula: inhibition rate (IR) = $[1-(OD_{treated}/OD_{control})\times100\%]$. Half maximal effective concentration (EC50) was calculated by non-linear regression fit of the mean values of the data obtained in triplicate independent experiments by GraphPad Prism 5.0 software (La Jalla, CA, USA). After determination of EC50 of BTZ and GNA, MM.1S cells were treated with both BTZ and GNA for 48h according to the ratio of EC50 of BTZ and GNA. The nature of drug interaction was analyzed by using the combination index (CI) according to the method of Chou and Talalay (1984). A CI<0.90 indicates synergism; a CI between 0.90 and 1.10 indicates additive, and a CI>1.10 indicates antagonism. Data analysis was performed by the Calcusyn software (Biosoft, Oxford, UK).

Cell cycle distribution analysis

Approximately 1×10^5 MM.1S cells were harvested at room temperature after pretreatment with various reagents for 48 or 72 h. The supernatant was removed and the cells were trypsinized and then ice-cold 70% ethanol was added. Ethanol-fixed cells were resuspended in PBS containing 0.1mg mL^{-1} RNase and incubated at 37°C for 30 min. The pelleted cells were suspended in 1.0mL of 40μg mL^{-1} propidium iodide (PI) and analyzed by using flow cytometer (Becton Dickinson, San Jose, CA, USA). The cell cycle distribution was estimated according to standard procedures. The percentage of cells in the different cell cycle phases (Sub G1, G1, S, or G2/M phase) were calculated using Flowjo (Becton Dickinson) software. The cells of sub G1 peak were considered apoptopic.

Apoptosis analysis

MM.1S cells were exposed to different concentrations of BTZ, GNA and combination treatment for 48h and 72h. After that, 1×10^5 cells were trypsinized with EDTA-free trypsogen, washed twice in PBS and resuspended in 400μL of 1×Binding Buffer. 5μL of Annexin V-FITC and 5μL PI were added to the cells. After incubation at room temperature for 15 minutes in the dark, cells were then analyzed by flow cytometer (Becton Dickinson, San Jose, CA, USA).

Western blot analysis

Approximately 1×10^7 MM.1S cells were gathered after pretreatment for 48h. The nuclear protein was prepared by a commercial kit (Thermo Scientific, Rockford, IL, USA). The tumor tissue protein was purified according to the reported method [25]. Equal amounts of total protein extracts from cultured cells or tissues were fractionated by 10-15% sodium dodecyl sulfate polyacrylamide gel electrophoresis (SDS-PAGE) and electrically transferred onto polyvinylidenedifluoride (PVDF) membranes. Mouse or rabbit primary antibodies and horseradish peroxidase (HRP)-conjugated appropriate secondary antibodies were used to detect the designated proteins. The bound secondary antibodies on the PVDF membrane were reacted with ECL detection reagents (Thermo Scientific) and exposed in ImageQuant LAS 4000mini system (GE Healthcare, Buckinghamshire, UK). Results were normalized to the internal control glyceraldehyde-3-phosphate dehydrogenase (GAPDH). Each experimental group was replicated 3 times. Image J analysis software was used to measure the bands intensity.

In vivo tumor growth model

Six-week-old male BALB/c nude mice, with body weights of 18-22g, were purchased from Slaccas Laboratary Animal Center (Shanghai, China) and maintained in a specific pathogen-free environment. The mice were subcutaneously injected with 1×10^7 cells. When the average tumor volume reached more than 100 mm^3, the mice were randomly divided into four groups, including control (DMSO only, d1, 3, 4, 5, 7, 8, 9, 11, 13; n=5), BTZ (0.25mg kg^{-1} d1, 4, 8, 11; n=5), GNA (2.0mg kg^{-1} per 2 days; n=5) and combination (0.25mg kg^{-1} BTZ d1, 4, 8, 11 plus 2.0mg kg^{-1} GNA per 2 days; n=5). Tumor size was measured once every 2 days with a caliper (calculated volume = shortest $diameter^2$ × longest diameter/2). Body weight of each mouse was recorded twice a day. After 14 days, the mice were sacrificed and the tumors were excised and stored at -80°C until further analysis. This study was performed in strict accordance with the recommendations in the Guide for the Care and Use of Laboratory Animals of the National Institutes of Health (NIH). The protocol was approved by the Committee on the Ethics of Animal Experiments of Medical School of Southeast University.

Apoptosis analysis by TUNEL

Formalin-fixed tumor tissues harvested 28 days after tumor implantation were embedded in paraffin

and sectioned. TUNEL was used to detect apoptosis in the tumor sections placed on slides according to the manufacturer's protocol. Tissue sections were analyzed to detect the localized green fluorescence of apoptotic cells and blue fluorescence of cell nuclei. Images were acquired and photographed using the Olympus IX51 fluorescence microscope (400×).

Immunohistochemistry

Immunohistochemical staining was performed using UltraSensitive S-P IHC (Maixin, Fuzhou, China) according to the manufacturer's protocols. The sections were incubated with anti-Ki-67, anti-cleaved PARP, anti-P53, anti-cleaved Caspase-3, anti-Bax or anti-Bcl-2 (1:100, Santa Cruz Biotechnology) at 4°C overnight. Then sections were stained with a streptavidin-peroxidase system, the signal was visualized using diaminobenzidine substrate and counterstaining was done with hematoxylin.

Statistical analysis

Statistical analysis was performed using SPSS 22.0 software package for Windows (SPSS, Chicago, IL, USA). Data were presented as the mean ± standard deviation (SD). Statistical significance was calculated using a Student's t-test, with a probability level of $P<0.05$ considered to be statistically significant, and $P<0.01$ considered to be highly significant.

Results

GNA synergized the growth inhibitory activity of BTZ on MM.1S cells

The growth inhibitory effects of BTZ or GNA on MM.1S cells were assessed by the CCK-8 assay after 24, 48 and 72 hour exposure. A concentration- and time-dependent inhibition of cell growth was observed with BTZ and GNA (Figure 1B), with EC50s of 5.024, 4.028 and 3.955nM of BTZ and 1.754, 0.900 and 0.839μM of GNA respectively. As the CI method recommends a ratio of EC50 values that ensures the agents are equipotent, combination studies were performed at fixed 1: 225 (BTZ: GNA) concentration ratio in MM.1S cells for 48h. The results showed that 48h of exposure to BTZ and GNA led to a strong synergistic antiproliferative activity on MM.1S cell lines (Figure 1C) with the maximal CI 0.753 with 4.0nM BTZ and 0.9μM GNA where inhibition rate was 73%. The predictive maximal CI was 0.786 with 2.3nM BTZ and 0.51μM GNA where inhibition rate was 55%. These results suggested that GNA may synergize the growth inhibitory activities of BTZ on MM.1S cells when co-administered.

Both BTZ and GNA triggered G2/M cell cycle arrest

Flow cytometry analysis after PI staining was used to detect the cell cycle arrest induced by BTZ, GNA and combination treatments. MM.1S cells were treated with BTZ and GNA at EC50 concentrations (pharmacologically achievable concentration), or combination of both for 48 h. As displayed in Figure 2A and Figure 2B, the percentages of MM.1S in G2/M phase after 48h of 2.3nM and 4.0nM BTZ treatment were 27.01±1.80% and 31.09±2.16% respectively. The percentages of MM.1S in G2/M phase after 48h of 0.51μM and 0.90μM GNA treatment were 23.19±1.44% and 26.68±1.96% respectively. The percentages of MM.1S in G2/M phase of combination treatment of 2.3nM BTZ plus 0.51μM GNA and 4.0nM BTZ plus 0.9μM GNA were 31.34±1.81% and 19.88±1.89% respectively. The percentage of MM.1S in G2/M phase of control group was 17.23±1.65%. The percentage of MM.1S in sub G1 phase after 48h 0.90μM GNA treatment was 30.23±0.66% and the percentage in sub G1 phase after 4.0nM BTZ plus 0.9μM GNA treatment was 34.93±3.09%. These results suggested that 4.0nM BTZ, 0.51μM GNA, 0.90μM GNA, and 2.3nM BTZ plus 0.51μM GNA for 48h could induce G2/M phase arrest significantly in MM.1S ($p<0.05$), whereas 0.9μM GNA and 4.0nM BTZ combined with 0.9μM GNA may induce apoptosis of MM.1S cells with high significance ($p<0.01$).

GNA enhanced the apoptosis-induced effect of BTZ on MM.1S cells

After treatment for 48h and 72h, MM.1S cells were stained with DAPI. Changes of cell nuclear morphology in exposed cells were observed by fluorescence microscopy, which revealed a marked increase in the quantity of apoptotic chromatin condensation and nuclear fragmentation depending on the concentrations of BTZ, GNA or BTZ plus GNA. An Annexin V-FITC/PI apoptosis detection kit was used to quantitatively determine whether BTZ, GNA or combined treatment induced apoptosis of MM.1S cells. The apoptosis induction effects were observed (Figure 3A and Figure 3B). The apoptosis rates of MM.1S cells for 48h in MM.1S cells were 6.57±0.15% in control group, 11.43±1.77% and 89.67±5.15% after treatment with 2.3nM and 4.0nM BTZ respectively; 7.06±0.04% and 97.80±0.81% after treatment with 0.51μM and 0.90μM GNA respectively; 25.37±1.71%, 98.9±3.86% after treatment with 2.3nM BTZ plus 0.51μM GNA, and 4.0nM BTZ plus 0.9μM GNA respectively. All the treatment groups showed a more significant apoptosis rate compared to that of the control group ($p<0.01$). All the combined groups showed a more significant apoptosis rate compared

with that of the single agent group of each accordingly (p<0.01). The apoptosis rates of MM.1S cells for 72h were 6.26±0.45% in control group, 78.16±3.65% and 98.50±2.62% after treatment with 2.3nM and 4.0nM BTZ respectively; 21.18±2.65% and 98.74±3.11% after treatment with 0.51μM and 0.90μM GNA respectively; 98.26±4.62% and 99.30±2.61% after treatment with 2.3nM BTZ plus 0.51μM GNA, and 4.0nM BTZ plus 0.9μM GNA respectively. As indicated in Figure 3C, all the treatment groups at 48 and 72 hours showed more significant apoptosis compared with that of the control group (p<0.01). Groups of 2.3nM BTZ plus 0.51μM GNA showed more significant apoptosis compared with that of the single agent group of each accordingly (p<0.01). Groups of 2.3nM BTZ, 0.51μM GNA,4.0nM BTZ, 2.3nM BTZ plus 0.51μM GNA and 4.0nM BTZ plus 0.9μM GNA at 48h showed less significant apoptosis compared with that of 72h of each accordingly (p<0.05). Clearly both BTZ and GNA were able to induce apoptosis in a dosage- and time-dependent manner in MM.1S cells.

The effects of combination of BTZ and GNA on apoptosis-related proteins

To further study the role of apoptosis induced by BTZ plus GNA, we evaluated the expression of PARP, P53, Caspase-3, Bax and Bcl-2 proteins by western blot performed on whole-cell lysates from control and treated MM.1S, presented in Figure 4. In MM.1S cells the combination treatment significantly increased PARP cleavages, P53, Caspase-3 cleavages and Bax proteins levels compared with BTZ and GNA alone (except the expression of Bax of 4.0nM BTZ plus 0.9μM GNA compared with 4.0nM BTZ and 0.9μM GNA) (p<0.05). The combination significantly decreased the expression of Bcl-2 compared with BTZ or GNA alone (p<0.01). These results demonstrate that the PARP, P53, Caspase-3, Bax and Bcl-2 proteins may also be involved in the synergism.

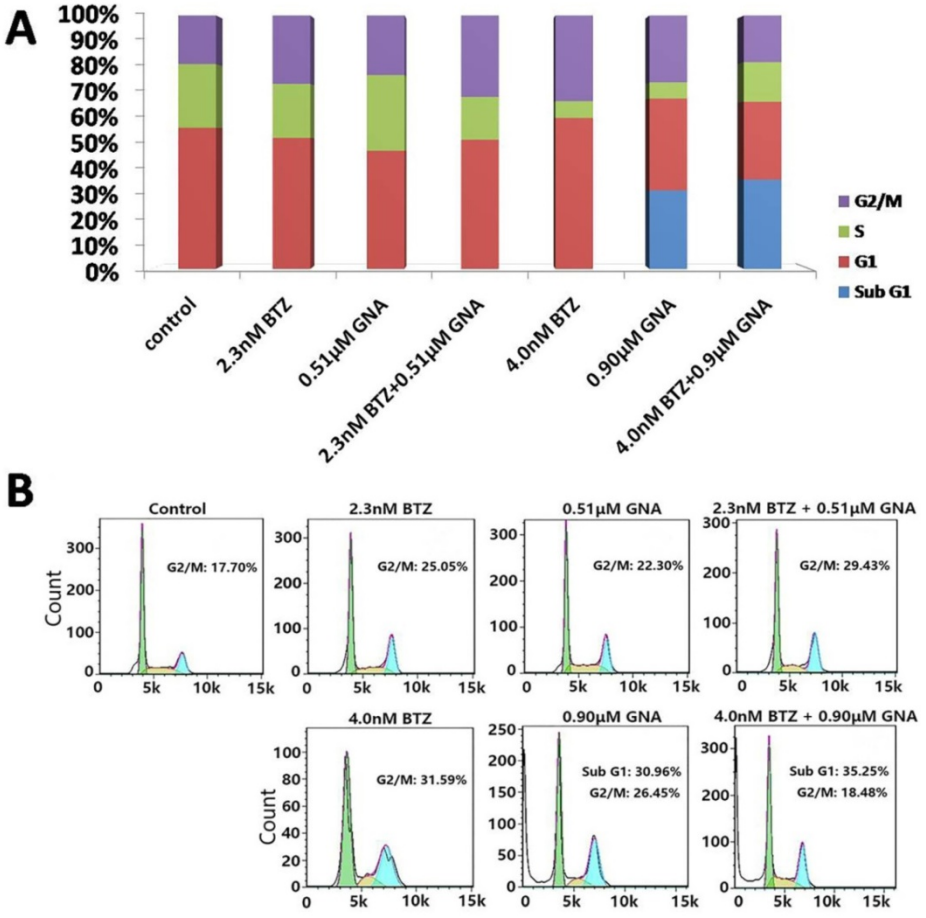

Figure 2. Apoptosis and cell cycle arrest of MM.1S cells induced by BTZ and GNA alone and combination assessed by flow cytometry analysis. (A) Distribution of MM.1S cells at different phases of the cell cycle. (B) Cells were exposed to 2.3nM BTZ, 0.51μM GNA alone and in combination, and 4.0nM BTZ, 0.90μM GNA alone and in combination for 48h, followed by analysis of cell cycle by flow cytometry. Sub G1 is considered as apoptosis.

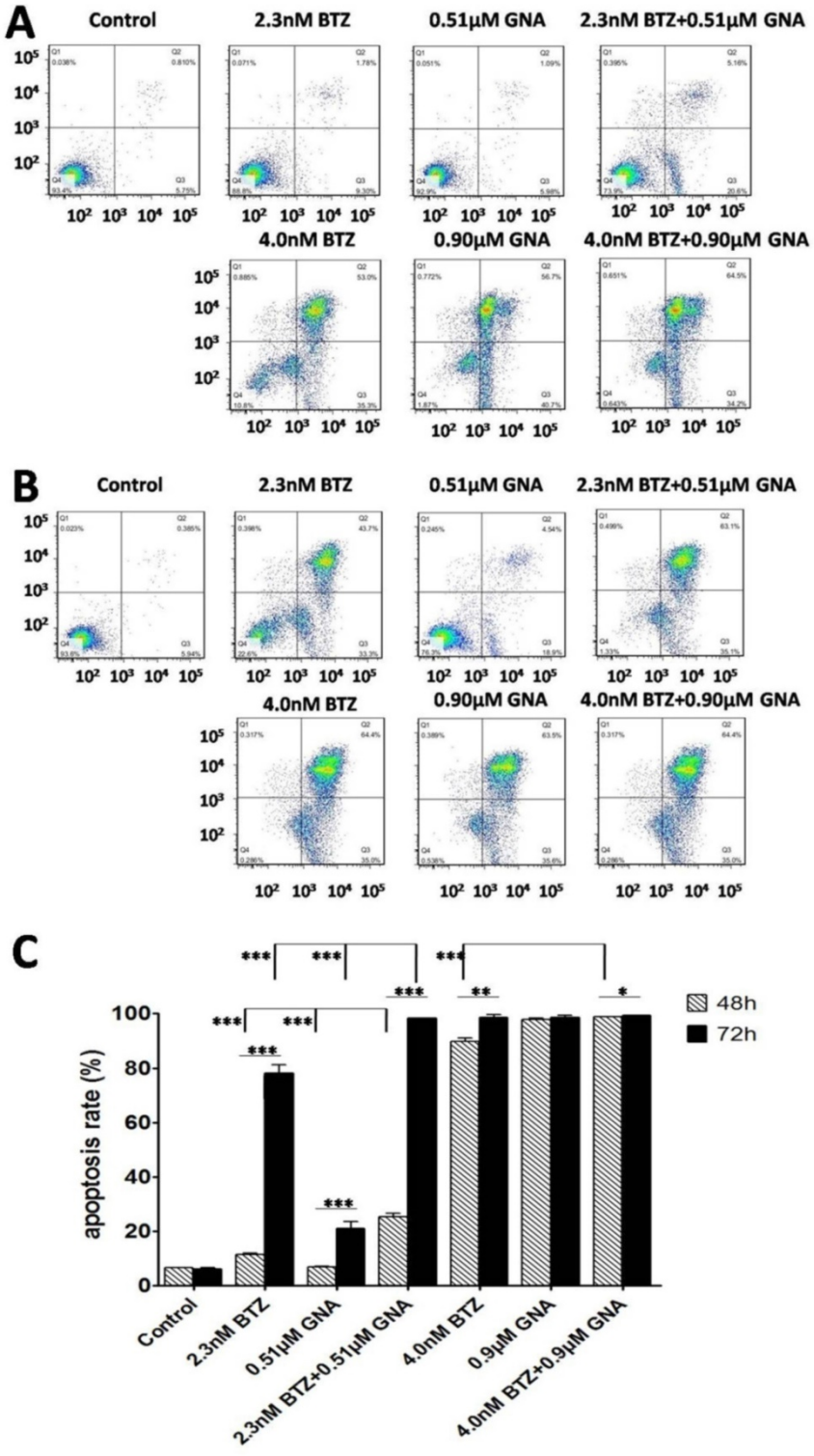

Figure 3. Combination of BTZ and GNA induced an enhancement of apoptosis by flow cytometry analysis. (A) MM.1S cells were treated with 2.3nM BTZ, 0.51μM GNA alone and in combination, and 4.0nM BTZ, 0.90μM GNA alone and in combination for 48h. (B) MM.1S cells were treated with 2.3nM BTZ, 0.51μM GNA alone and in combination, and 4.0nM BTZ, 0.90μM GNA alone and in combination for 72h. (C) The apoptosis rate was processed statistically. Columns, means for three replicate determinations; bars, s.d. **P*<0.05, ***P*<0.01, ****P*<0.001.

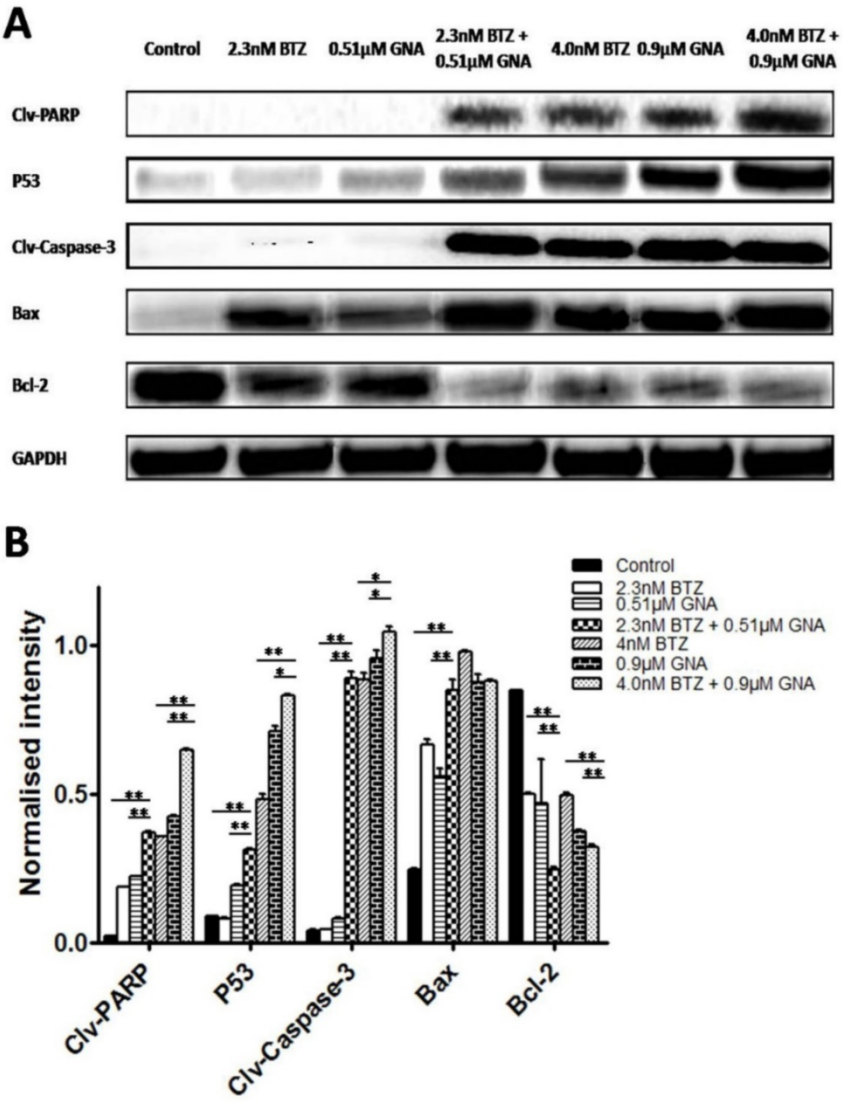

Figure 4. Effects of BTZ, GNA and the combination on apoptosis-related proteins of MM.1S cells. MM.1S cells were treated with DMSO control, BTZ, GNA, or combination of two concentrations, respectively. (A) Western blot analysis of BTZ and GNA-induced PARP, P53, Caspase-3, Bax and Bcl-2 levels in MM.1S for 48h. (B) The normalized intensity of cleaved PARP, P53, cleaved Caspase-3, Bax and Bcl-2 proteins were processed statistically. DMSO, dimethyl sulfoxide. Columns, means for three replicate determinations; bars, s.d. **P*<0.05, ***P*<0.01.

The combination of BTZ and GNA inhibited tumor growth *in vivo*

To investigate whether GNA synergizes BTZ against tumor growth *in vivo*, MM.1S tumors were implanted in BALB/C nude male mice. It was observed that the mice consumed less food and were less physically active during the study. At the end of the experiment all mice were sacrificed (Figure 5C). The body weights of treatment groups showed no significant loss as compared with mice in the control group (Figure 5A). The tumor volume of combination-treated mice showed a slight but not significant difference as compared with that in the control group, BTZ group and GNA group (Figure 5B). The tumor weights were found to have all decreased, whereas the degree of tumor reduction differed (Figure 5D). For the control group the mean tumor weight was 0.62g at the end of the experiment, whereas the mean tumor weights were 0.56g in BTZ group and 0.50g in GNA group, and 0.36g in BTZ plus GNA group at the end of the experiment. The tumor weights of GNA and BTZ plus GNA groups decreased significantly when compared with those of control group ($p<0.01$ and $p<0.001$, respectively) and the tumor weight of combination group was significantly less than that of BTZ or GNA group ($p<0.001$). When mice were treated with BTZ combined with GNA, the tumor inhibition rate was 41.94%, whereas those of mice treated with BTZ or GNA alone were 9.68% and 19.35%, respectively. These results demonstrate that the antitumor effect of BTZ combined with GNA is superior to that of the single agents used individually. Thus, our data

suggests that the combination of BTZ and GNA produced much more potent tumor growth inhibitory effects, without increasing the toxicities to the animals.

The combination of BTZ and GNA induced apoptosis, upregulated PARP cleavage, P53, Caspase-3 cleavage and Bax , and downregulated Ki-67 and Bcl-2 in tumor tissues

To explore the underlying mechanisms of the synergistic effect *in vitro*, the effect of single agent or combined treatment of BTZ and GNA on the apoptosis and the expression levels of apoptosis-related proteins in tumor tissues from drug-administered mice were further assessed.

Samples were analyzed to detect the localized green fluorescence of apoptotic cells and blue fluorescence of cell nuclei using a fluorescence microscope by TUNEL assay (Figure 6B). The percentage of apoptotic cells compared to the average number of cells per field was determined and graphically represented (Figure 6A). As can be seen, the combination therapy induced an enhanced apoptosis in the tumor tissues from the mice. The apoptotic rate in single agent groups and combined treatment group increased significantly compared with that of the control group ($p<0.001$).The apoptosis rate in combined treatment groups increased significantly compared with that of BTZ or GNA alone ($p<0.05$; $p<0.01$).

To investigate and address the potential effect of BTZ and GNA *in vivo*, immunohistochemistry was performed (Figure 7A and Figure 7B). The results showed that the presence of Ki-67 and Bcl-2 in xenografts were most reduced in BTZ and GNA combination treatments, while least reduced in the control group ($p<0.001$). PARP cleavage, P53, Caspase-3 cleavage and Bax were most expressed in the combined group, while least expressed in the control group ($p<0.001$). The result suggests that BTZ and GNA had synergistic effects on apoptosis.

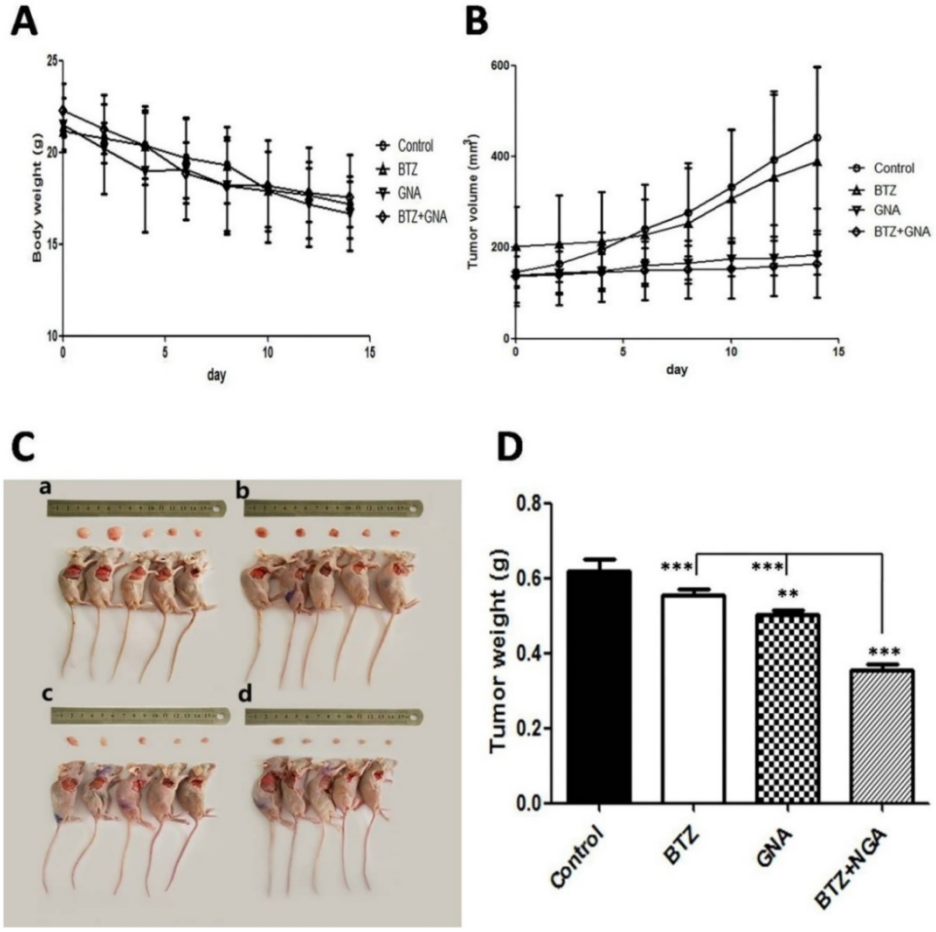

Figure 5. The antitumor effect of BTZ and GNA on MM.1S xenograft models. (A) The mice transplanted with MM.1S xenografts were randomly divided into four groups and given injection intravenously of BTZ (0.25mg kg^{-1} d1, 4, 8, 11), GNA (2.0mg kg^{-1} per 2 days) and combination (0.25mg kg^{-1} BTZ d1, 4, 8, 11 plus 2.0mg kg^{-1} GNA per 2 days) or vehicle for a period of 2 weeks. The average body weight of each group is expressed as mean±s.d. (n=5 per group). (B) The tumor volumes are expressed as mean ±s.d. (n=5 per group). (C) After 14 days, tumors of each group were dissected and photographed: (a) control group, (b) BTZ group, (c) GNA group and (d) BTZ + GNA group. (D) Average tumor weight of each group at the end of experiments. Columns, means for three replicate determinations; bars, s.d. ***P*<0.01, ****P*<0.001.

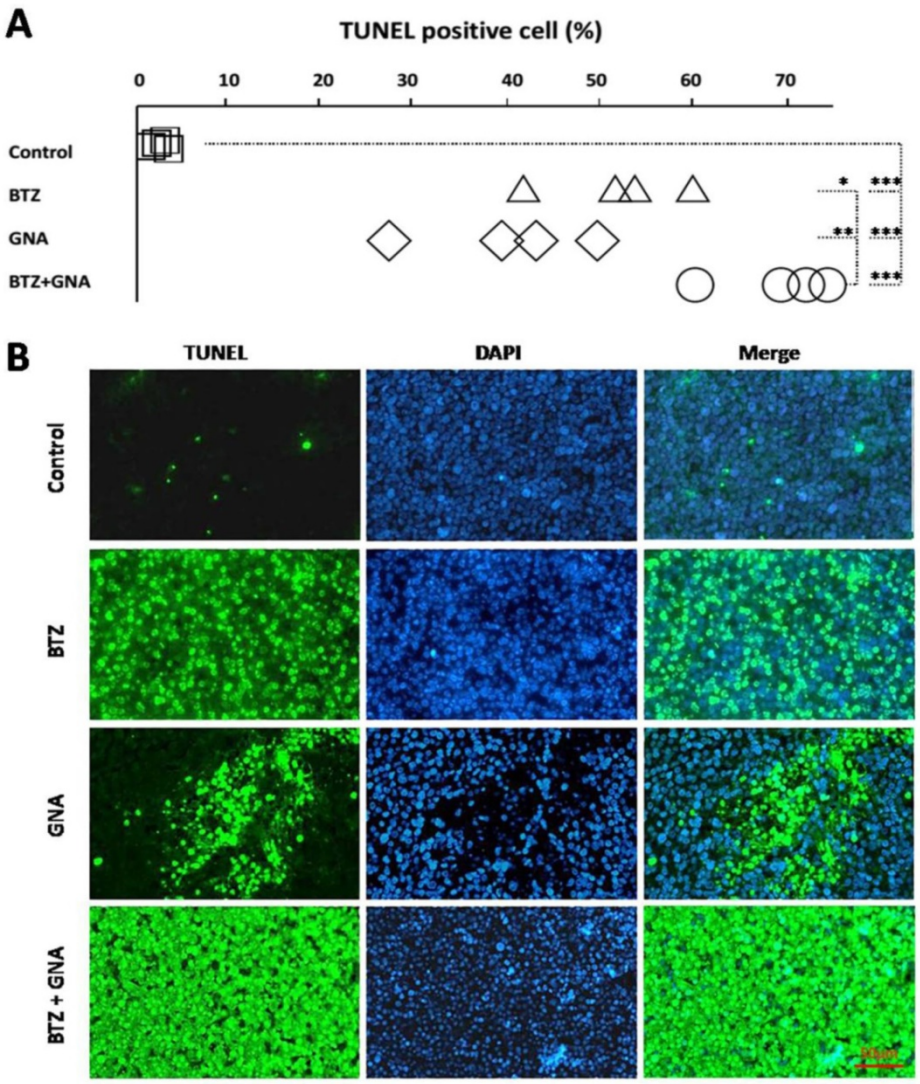

Figure 6. Analysis of apoptosis by TUNEL staining in tumor tissues in different groups (n = 5).The TUNEL assay revealed apoptotic-positive hepatic cells marked by green staining. The blue DAPI stain marks intact DNA. Magnification, ×400. TUNEL, terminal deoxynucleotidyl transferase dUTP nick end-labeling; DAPI, 4'6'-diamidino-2-phenylindole dihydrochloride. *P<0.05, **P<0.01, ***P<0.001.

Western blot of tumor tissues was performed in order to address the mechanism of apoptosis (Figure 8A and Figure 8B). The results showed that the combination treatment significantly increased cleaved PARP, P53, cleaved Caspase-3 and Bax proteins levels compared with BTZ or GNA alone and control group (p<0.01). The combination group significantly decreased expression of Ki-67 and Bcl-2 compared with BTZ or GNA alone and control group (p<0.01). These results demonstrate that the PARP, P53, Caspase-3, Bax and Bcl-2 proteins were also involved in the synergism *in vivo*. These results further support that GNA synergistically potentiates bortezomib-induced apoptosis in MM and that combined therapy of BTZ and GNA could be a potential chemotherapy regimen for MM.

Discussion

In this study, the synergistic collaboration between BTZ and GNA inducing apoptosis of myeloma MM.1S cells *in vitro* and *in vivo* was illustrated for the first time, evidenced by the activation of apoptosis-related proteins. Furthermore, GNA was found to act synergistically with BTZ to reduce the tumor burden in the MM.1S xenograft model. Importantly, we explored the underlying mechanisms of apoptosis induction and BTZ sensitization by GNA, which involves proteins such as PARP, P53, Caspase-3, Bax and Bcl-2.

BTZ is one of the most widely used agents in the current therapy for MM [26-28]. It exerts its potent anti-myeloma activity in two predominant ways: upregulation of the proapoptotic protein NOXA,

which may interact with the anti-apoptotic proteins of Bcl-2 subfamily Bcl-X(L) and Bcl-2 and result in apoptotic cell death in malignant cells; suppression of the NF-kappa B signaling pathway resulting in the down-regulation of its anti-apoptotic target genes [29]. BTZ has demonstrated significant activity in clinical trials for MM; however, resistance to BTZ still remains a clinically significant problem [8, 30, 31]. In addition, the dose-limiting toxicities such as peripheral neuropathy of BTZ caused deleterious effect on MM patients [27, 32]. As a promising anticancer agent with multiple protein targets, GNA was reported to induce apoptosis of cancer cells through both death receptor and mitochondrial apoptotic pathways [18, 22, 23]. To date, studies reporting the use of these two agents in combination have not been reported. It is important to highlight that our study is the first to extensively to investigate the *in vitro* and *in vivo* effects of combing low concentrations of BTZ and GNA in MM.1S cells.

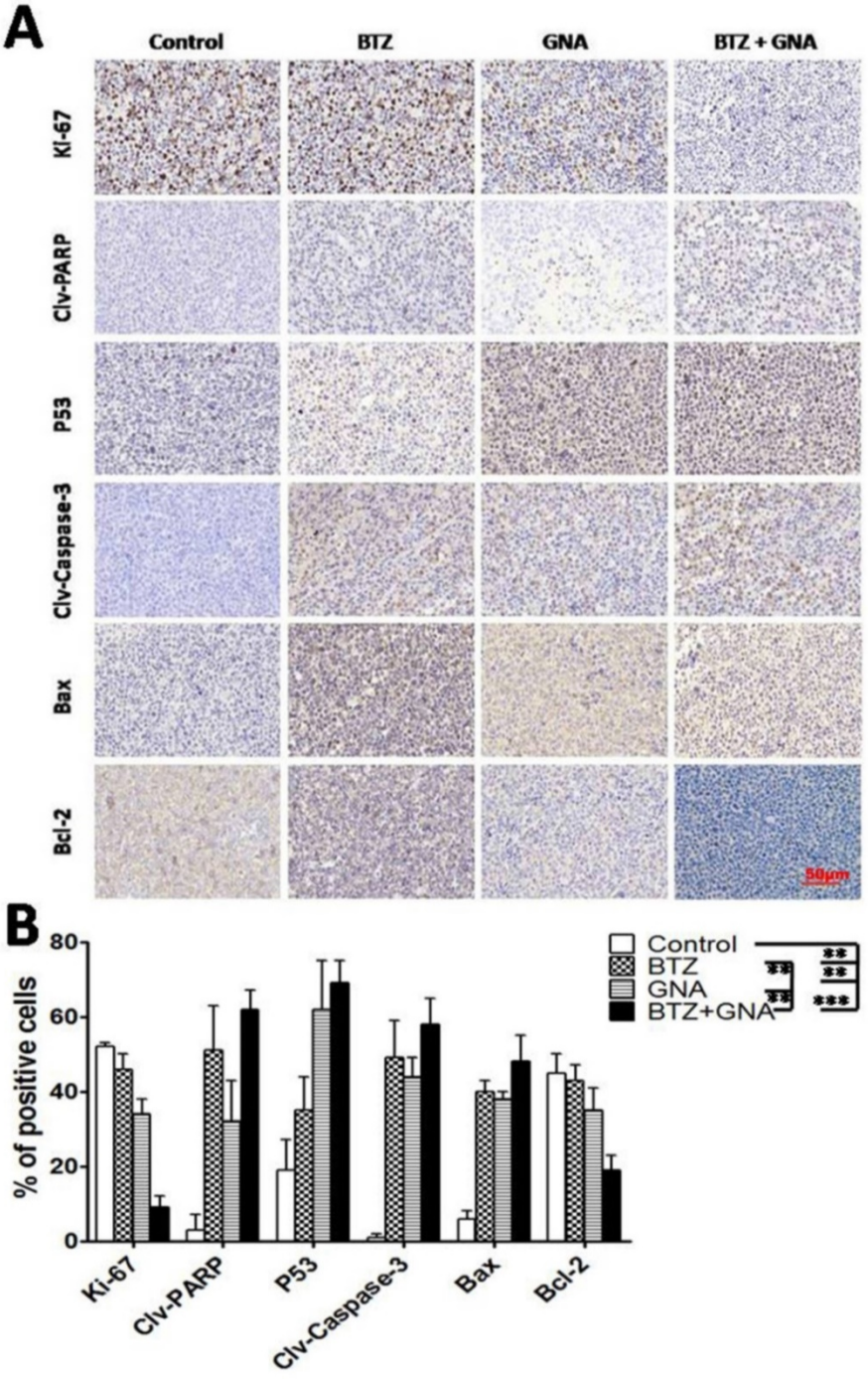

Figure 7. Representative photographs of immunochemistry of Ki-67, PARP cleavage, P53, Caspase-3 cleavage, Bax and Bcl-2 in different groups. Staining was performed with anti-ki-67 antibody for proliferation, anti-PARP cleavage, -P53, Caspase-3 cleavage, -Bax and -Bcl-2 polyclonal antibodies for apoptosis. Magnification, ×400. Columns, means of four quadrants of positive cells; bars, s.d. $^{**}P<0.01$, $^{***}P<0.001$.

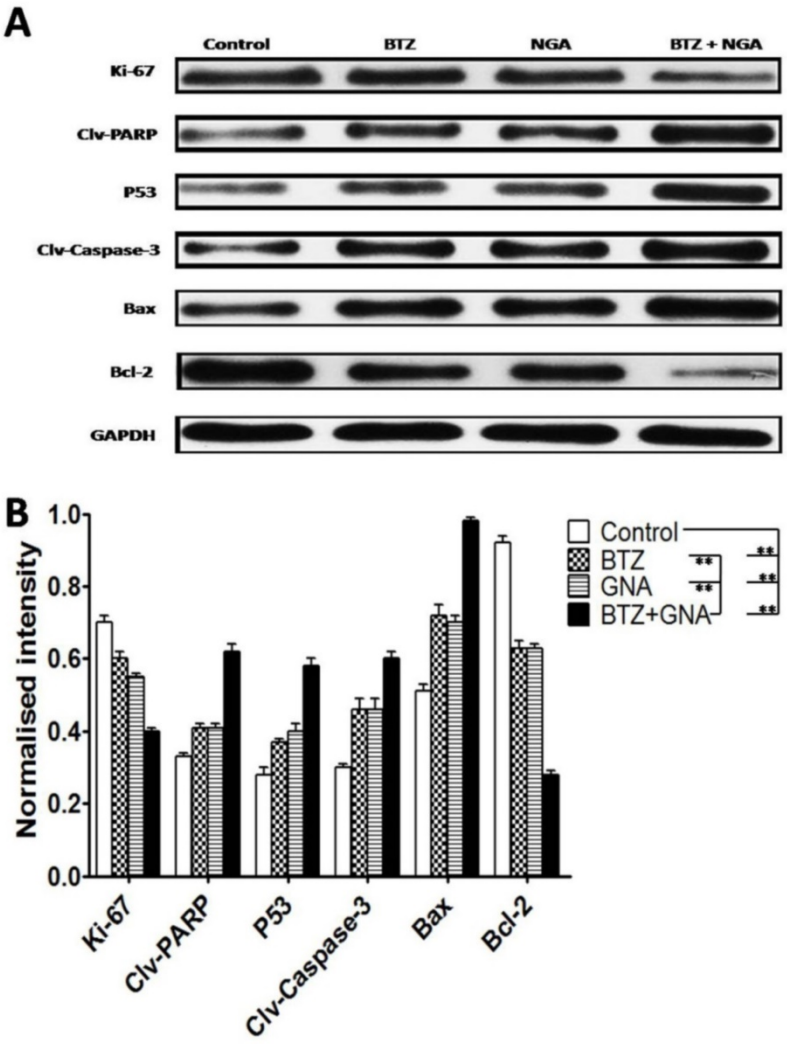

Figure 8. Western blot analysis of BTZ, GNA and the combination on apoptosis-related proteins of tumor tissues. (A) Western blot analysis of Ki-67, PARP cleavage, P53, Caspase-3 cleavage, Bax and Bcl-2. The protein expression levels (relative to GAPDH) were assessed. (B) The normalized intensity of cleaved PARP, P53, cleaved Caspase-3, Bax and Bcl-2 proteins were processed statistically. Columns, means for three replicate determinations; bars, s.d. **P*<0.05, ***P*<0.01, ****P*<0.001.

In this study, CCK-8 assay indicated that both BTZ and GNA exhibited evident cytotoxicity to multiple myeloma MM.1S cells in time- and dose-dependent manner. Also, our results showed that BTZ and GNA combination were observed to act synergistically to induce apoptosis inMM.1S cells.

Apoptosis, programmed cell death, is one of the most important anticancer mechanisms [33]. The classic apoptotic morphologic changes include condensation of chromatin, nuclear fragmentation and apoptotic bodies [34-36]. In this study, apoptosis was observed by DAPI staining after cells were treated by BTZ and GNA. Our results demonstrated that both BTZ and GNA induced MM.1S cells apoptosis in a dose- and time-dependent manners by FACS. Besides, *in vivo* TUNEL test has also demonstrated that both these agents induced apoptosis of MM.1S cells.

Cell cycle arrest is one of the mechanisms for cell growth inhibition induced by many anticancer drugs. Our results demonstrated that GNA could promote BTZ inducing G2/M-phase cell cycle arrest in MM.1S cells. Inducing G2/M-phase cell cycle arrest of BTZ has been reported by several studies [37-39]. However, that GNA could induce G2/M phase arrest of MM.1S cells was first demonstrated in this study. It is worth noting that previous studies about cell cycle arrest induced by GNA were not consistent. Several studies indicated that GNA could induce G1 arrest in lung cancer A549 cells [16, 21, 40] and breast cancer MCF-7 cells [22], but the study conducted by Chen *et al* [19] confirmed that GNA can induce cell cycle arrest of MCF-7 cells at the G2/M phase. Hence, further study of the cell cycle arrest process of MM.1S by GNA is needed.

Although treatment with BTZ or GNA alone induced apoptosis in MM.1S cells and decreased their proliferation, these effects were more pronounced

when BTZ and GNA were simultaneously utilized to treat the cells. Consistent with the occurrence of apoptotic cell death, BTZ or GNA alone increased levels of PARP cleavage, P53, Caspase-3 cleavage and Bax, and decreased Bcl-2 levels, these effects increased significantly with the combined treatment as observed via western blot.

We also studied the effects of BTZ and GNA, alone or in combination, *in vivo* using nude mice with MM.1S cell-driven xenografts. Combining low doses of BTZ (0.25mgkg^{-1} d1,4,8,11) and GNA (2.0 mg kg^{-1} per two days) suppressed the growth of MM.1S cell xenografts more efficiently than either drug alone. In addition, apoptosis was more evident in MM.1S myeloma collected from mice treated simultaneously with BTZ and GNA than mice treated with either drug alone observed by assay of TUNEL, immunochemistry and western blot. It is important to highlight that apparent toxicity was not observed in the nude mice because of the relatively low doses of GNA and BTZ that were intermittently administered in our model. The above data demonstrated that GNA might become an ideal agent for combination treatment with BTZ and may help overcoming BTZ resistance and reduce toxicities when BTZ use in MM patients.

The identification of optimal dosing regimens and schedules is necessary for evaluating cancer therapeutics in clinical study, especially when therapies are combined [11, 41-43]. Preclinical results are valuable to guide the design of clinical study protocols. In summary, we verified for the first time that GA could potentiate the execution of apoptosis of MM.1S cells triggered by BTZ *in vitro* and *in vivo* via several apoptosis related proteins including PARP, P53, Caspase-3, Bax and Bcl-2.

Taken together, these data suggest that the combination of BTZ and GNA is an attractive novel potential therapy for the treatment of MM. Importantly, the findings observed *in vitro* were consistent with those observed *in vivo*, which supports the efficacy of this approach and provides legitimate rationale for clinical utilization to treat patients with MM in the future. Further studies are warranted to investigate the specific mechanisms and efficacy of the BTZ-GNA combination in the clinical settings during therapy for MM.

Acknowledgments

We gratefully acknowledge the financial support from the National Natural Science Foundation of China (81370673) and Key Medical Project of Jiangsu Province (BL2014078). Sincere gratitude should be given to Dr. Jos L Campbell for his careful English editing.

Author's contributions

R.C., H.Z. and B.C. performed experiments and analyzed data; R.C. and B.C. designed the experiments; P. L and X.W. did the data analysis; R.C. and B.C. wrote the manuscript.

Competing Interests

The authors have declared that no competing interest exists.

References

1. San Miguel JF. Introduction to a series of reviews on multiple myeloma. Blood. 2015; 125: 3039-40.
2. Shaughnessy JD, Jr., Qu P, Usmani S, Heuck CJ, Zhang Q, Zhou Y, et al. Pharmacogenomics of bortezomib test-dosing identifies hyperexpression of proteasome genes, especially PSMD4, as novel high-risk feature in myeloma treated with Total Therapy 3. Blood. 2011; 118: 3512-24.
3. Moreau P, Attal M, Facon T. Frontline therapy of multiple myeloma. Blood. 2015; 125: 3076-84.
4. Moreau P, Richardson PG, Cavo M, Orlowski RZ, San Miguel JF, Palumbo A, et al. Proteasome inhibitors in multiple myeloma: 10 years later. Blood. 2012; 120: 947-59.
5. Blade J, Rosinol L, Cibeira MT, Rovira M, Carreras E. Hematopoietic stem cell transplantation for multiple myeloma beyond 2010. Blood. 2010; 115: 3655-63.
6. Driscoll J. Expression of E3 Ubiquitin Ligases in Multiple Myeloma Patients after Treatment with the Proteasome Inhibitor Bortezomib. Cancer Trans Med. 2015; 1: 153-7.
7. Chen R, Chen B, Zhang X, Gao C. Efficacy of carfilzomib in the treatment of relapsed and (or) refractory multiple myeloma: a meta-analysis of data from clinical trials. Discov Med. 2016; 22: 189-99.
8. Turner JG, Dawson J, Emmons MF, Cubitt CL, Kauffman M, Shacham S, et al. CRM1 Inhibition Sensitizes Drug Resistant Human Myeloma Cells to Topoisomerase II and Proteasome Inhibitors both In Vitro and Ex Vivo. J Cancer. 2013; 4: 614-25.
9. Nooka AK, Kastritis E, Dimopoulos MA, Lonial S. Treatment options for relapsed and refractory multiple myeloma. Blood. 2015; 125: 3085-99.
10. Fall DJ, Stessman H, Patel SS, Sachs Z, Van Ness BG, Baughn LB, et al. Utilization of translational bioinformatics to identify novel biomarkers of bortezomib resistance in multiple myeloma. J Cancer. 2014; 5: 720-7.
11. Zhang W, Qiao L, Wang X, Senthilkumar R, Wang F, Chen B. Inducing cell cycle arrest and apoptosis by dimercaptosuccinic acid modified Fe3O4 magnetic nanoparticles combined with nontoxic concentration of bortezomib and gambogic acid in RPMI-8226 cells. Int J Nanomed. 2015; 10: 3275-89.
12. Zhao Y, Sun Y, Ding Y, Wang X, Zhou Y, Li W, et al. GL-V9, a new synthetic flavonoid derivative, ameliorates DSS-induced colitis against oxidative stress by up-regulating Trx-1 expression via activation of AMPK/FOXO3a pathway. Oncotarget. 2015; 6: 26291-307.
13. Lin N, Mao X, Zhang Y. Application and Perspectives of Traditional Chinese Medicine in the Treatment of Liver Cancer. Cancer Trans Med. 2015; 1: 101-7.
14. Wang Z, Liu X, Ho RL, Lam CW, Chow MS. Precision or Personalized Medicine for Cancer Chemotherapy: Is there a Role for Herbal Medicine. Molecules. 2016; 21.
15. Song JZ, Yip YK, Han QB, Qiao CF, Xu HX. Rapid determination of polyprenylated xanthones in gamboge resin of Garcinia hanburyi by HPLC. J Sep Sci. 2007; 30: 304-9.
16. Li Q, Cheng H, Zhu G, Yang L, Zhou A, Wang X, et al. Gambogenic acid inhibits proliferation of A549 cells through apoptosis-inducing and cell cycle arresting. Biol Pharm Bull. 2010; 33: 415-20.
17. Lin T, Fang Q, Peng D, Huang X, Zhu T, Luo Q, et al. PEGylated non-ionic surfactant vesicles as drug delivery systems for Gambogenic acid. Drug Deliv. 2013; 20: 277-84.
18. Chen HB, Zhou LZ, Mei L, Shi XJ, Wang XS, Li QL, et al. Gambogenic acid-induced time- and dose-dependent growth inhibition and apoptosis involving Akt pathway inactivation in U251 glioblastoma cells. J Nat Med. 2012; 66: 62-9.
19. Chen F, Zhang XH, Hu XD, Zhang W, Lou ZC, Xie LH, et al. Enhancement of radiotherapy by ceria nanoparticles modified with neogambogic acid in breast cancer cells. Int J Nanomed. 2015; 10: 4957-69.
20. Yu XJ, Zhao Q, Wang XB, Zhang JX, Wang XB. Gambogenic acid induces proteasomal degradation of CIP2A and sensitizes hepatocellular carcinoma to anticancer agents. Oncol Rep. 2016; 36:3611-8.
21. Cheng H, Su JJ, Peng JY, Wang M, Wang XC, Yan FG, et al. Gambogenic acid inhibits proliferation of A549 cells through apoptosis inducing through up-regulation of the p38 MAPK cascade. J Asian Nat Prod Res. 2011; 13: 993-1002.
22. Wang K, Tang Y, Sun M, Lu B, Zhu H, Ji O, et al. The mechanism of neogambogic acid-induced apoptosis in human MCF-7 cells. Acta Bioch Bioph Sin. 2011; 43: 698-702.

23. Zhou J, Luo YH, Wang JR, Lu BB, Wang KM, Tian Y. Gambogenic acid induction of apoptosis in a breast cancer cell line. Asian Pac J Cancer Prev. 2013; 14: 7601-5.
24. Su J, Cheng H, Zhang D, Wang M, Xie C, Hu Y, et al. Synergistic effects of 5-fluorouracil and gambogenic acid on A549 cells: activation of cell death caused by apoptotic and necroptotic mechanisms via the ROS-mitochondria pathway. Biol Pharm Bull. 2014; 37: 1259-68.
25. Wang LH, Yang JY, Yang SN, Li Y, Ping GF, Hou Y, et al. Suppression of NF-kappaB signaling and P-glycoprotein function by gambogic acid synergistically potentiates adriamycin -induced apoptosis in lung cancer. Curr Cancer Drug Targets. 2014; 14: 91-103.
26. Kouroukis TC, Baldassarre FG, Haynes AE, Imrie K, Reece DE, Cheung MC. Bortezomib in multiple myeloma: systematic review and clinical considerations. Current Oncol. 2014; 21: e573-603.
27. Einsele H. Bortezomib. Recent Results Cancer Res. 2014; 201: 325-45.
28. Mohty M, Malard F, Mohty B, Savani B, Moreau P, Terpos E. The effects of bortezomib on bone disease in patients with multiple myeloma. Cancer. 2014; 120: 618-23.
29. Chen D, Frezza M, Schmitt S, Kanwar J, Dou QP. Bortezomib as the first proteasome inhibitor anticancer drug: current status and future perspectives. Curr Cancer Drug Targets. 2011; 11: 239-53.
30. Ruschak AM, Slassi M, Kay LE, Schimmer AD. Novel proteasome inhibitors to overcome bortezomib resistance. J Nat Cancer Inst. 2011; 103: 1007-17.
31. Argyriou AA, Iconomou G, Kalofonos HP. Bortezomib-induced peripheral neuropathy in multiple myeloma: a comprehensive review of the literature. Blood. 2008; 112: 1593-9.
32. Mujtaba T, Dou QP. Advances in the understanding of mechanisms and therapeutic use of bortezomib. Discov Med. 2011; 12: 471-80.
33. Johnstone RW, Ruefli AA, Lowe SW. Apoptosis: a link between cancer genetics and chemotherapy. Cell. 2002; 108: 153-64.
34. Kale J, Liu Q, Leber B, Andrews DW. Shedding light on apoptosis at subcellular membranes. Cell. 2012; 151: 1179-84.
35. Spencer SL, Sorger PK. Measuring and modeling apoptosis in single cells. Cell. 2011; 144: 926-39.
36. Fuchs Y, Steller H. Programmed cell death in animal development and disease. Cell. 2011; 147: 742-58.
37. Tamura D, Arao T, Tanaka K, Kaneda H, Matsumoto K, Kudo K, et al. Bortezomib potentially inhibits cellular growth of vascular endothelial cells through suppression of G2/M transition. Cancer Sci. 2010; 101: 1403-8.
38. Rapino F, Naumann I, Fulda S. Bortezomib antagonizes microtubule-interfering drug-induced apoptosis by inhibiting G2/M transition and MCL-1 degradation. Cell Death Dis. 2013; 4: e925.
39. Zhang J, Chen B, Wu T, Wang Q, Zhuang L, Zhu C, et al. Synergistic Effect and Molecular Mechanism of Homoharringtonine and Bortezomib on SKM-1 Cell Apoptosis. PloS one. 2015; 10: e0142422.
40. Yu XJ, Han QB, Wen ZS, Ma L, Gao J, Zhou GB. Gambogenic acid induces G1 arrest via GSK3beta-dependent cyclin D1 degradation and triggers autophagy in lung cancer cells. Cancer lett. 2012; 322: 185-94.
41. Moon du G, Lee SE, Oh MM, Lee SC, Jeong SJ, Hong SK, et al. NVP-BEZ235, a dual PI3K/mTOR inhibitor synergistically potentiates the antitumor effects of cisplatin in bladder cancer cells. Int J Oncol. 2014; 45: 1027-35.
42. Park J, Ayyappan V, Bae EK, Lee C, Kim BS, Kim BK, et al. Curcumin in combination with bortezomib synergistically induced apoptosis in human multiple myeloma U266 cells. Mol Oncol. 2008; 2: 317-26.
43. Qiao Z, He M, He MU, Li W, Wang X, Wang Y, et al. Synergistic antitumor activity of gemcitabine combined with triptolide in pancreatic cancer cells. Oncol Lett. 2016; 11: 3527-33.